Journal of Alloys and Compounds 513 (2012) 580–585

Contents lists available at SciVerse ScienceDirect

Journal of Alloys and Compounds

journal homepage: www.elsevier.com/locate/jallcom

Influence of processing conditions on the grain growth and electrical properties of barium zirconate titanate ferroelectric ceramics

Priyanka Arora Jha, A.K. Jha*

Thin Film & Material Science Laboratory, Department of Applied Physics, Delhi Technological University (Formerly Delhi College of Engineering), Bawana Road, Delhi 110042, India

ARTICLE INFO

Article history:
Received 13 July 2011
Received in revised form 31 October 2011
Accepted 2 November 2011
Available online 9 November 2011

Keywords:
Ceramics
Ferroelectrics
Sintering
Dielectric response
X-ray diffraction
Scanning electron microscopy
SEM

ABSTRACT

In this study, structural, dielectric and ferroelectric properties of $BaZr_{0.025}Ti_{0.975}O_3$ ferroelectric ceramics have been investigated. The compound was synthesized using solid state reaction technique. It is observed that the synthesized compound have perovskite crystal structure. As the sintering temperature increases from 1200 °C to 1250 °C and 1300 °C, the average grain size increases from 0.62 μm to 2.82 μm and 3.20 μm respectively. Moreover, the domains with "water-mark" and "lamellar" features are observed in SEM micrographs. The dielectric measurements as a function of temperature show a decrease in Curie temperature on increasing the sintering temperature. The decrease in Curie temperature is attributed to the decreased tolerance factor of the perovskite ABO_3 structure. There is enormous increase in the permittivity with the increase in grain size. The coercive field decreases and the remanent polarization increases as the grain size increases.

1. Introduction

In the past years, Pb-based materials have been widely studied due to their excellent ferroelectric, dielectric and piezoelectric properties. However, these materials possess some serious drawbacks when heat treated in the range of 500–900 °C due to the volatility and toxicity involved with the Pb containing compounds [1–4]. For environment friendly applications, researchers have been working for alternative to Pb-based materials. Since the discovery of barium titanate ($BaTiO_3$) in early 1940s, this material has been used for a wide range of scientific and industrial applications such as capacitors ultrasonic transducers, pyroelectric infra red sensors, etc. [5–8]. In order to reduce the dielectric loss at low frequencies, SrO and ZrO_2 have been used as a substituent as Zr^{+4} is chemically more stable than Ti^{+4} and has a larger ionic size to expand the lattice [9]. In case of barium titanate, Ti^{+4} reduces to Ti^{+3} and conduction by electron hopping takes place and conduction is depressed with the substitution of Zr^{+4} [10–14]. Barium zirconate titanate (BZT) shows a very large dielectric constant because of the pinching effect. Pinching effect occurs when the three phase transition temperatures of $BaTiO_3$ (T_1 = 198 K: rhombohedral to orthorhombic; T_2 = 273 K: orthorhombic to tetragonal; T_3 = 393 K: tetragonal to cubic) coexist [15]. The electrical properties exhibited by this material arise from lattice expansion effect [16]. In this report, the effect of sintering temperature on the structure, grain size and electrical properties of $BaZr_{0.025}Ti_{0.975}O_3$ is reported.

2. Experimental

Polycrystalline samples of composition $BaZr_{0.025}Ti_{0.975}O_3$ were prepared by the solid state reaction method by taking high purity $BaCO_3$, TiO_2 and ZrO_2 (all from M/s Aldrich, USA) in their stoichiometric proportions. The powder mixtures were thoroughly ground in an agate mortar and passed through a sieve of appropriate size. The powder mixture was then calcined at 1150 °C for 2 h in an alumina crucible. The calcined mixtures were ground and admixed with polyvinyl alcohol (PVA) as a binder and then pressed at 150 MPa into disk shaped pellets. The pellets were then sintered at 1200 °C, 1250 °C and 1300 °C for 2 h in air. X-ray diffractograms of all the sintered samples were recorded using a Bruker X-ray diffractometer with CuKα (λ = 1.5406 Å) radiations in the range $10° \leq 2\theta \leq 70°$ at a scanning rate of 2°/min. The microstructural studies of the samples were carried out using Scanning Electron Microscope (Hitachi S-3700 N). The sintered pellets were polished to a thickness of 1 mm and coated with silver paste on both sides to act as electrodes and then finally cured at 300 °C for 30 min. The dielectric measurements were carried out in the temperature range of room temperature to 300 °C at 10 kHz using a high precision LCR meter (HP 4284A) at an oscillation amplitude of 1 V. *P–E* hysteresis loops were recorded at room temperature using a *P–E* loop tracer based on Sawyer-Tower circuit.

3. Results and discussions

3.1. XRD analysis

X-ray diffractograms of the studied specimens are shown in Fig. 1. Lattice parameters were calculated from the diffractograms

* Corresponding author. Tel.: +91 98 68 24 21 50; fax: +91 11 27 87 10 23.
E-mail address: dr_jha_ak@yahoo.co.in (A.K. Jha).

0925-8388/$ – see front matter © 2011 Elsevier B.V. All rights reserved.
doi:10.1016/j.jallcom.2011.11.012

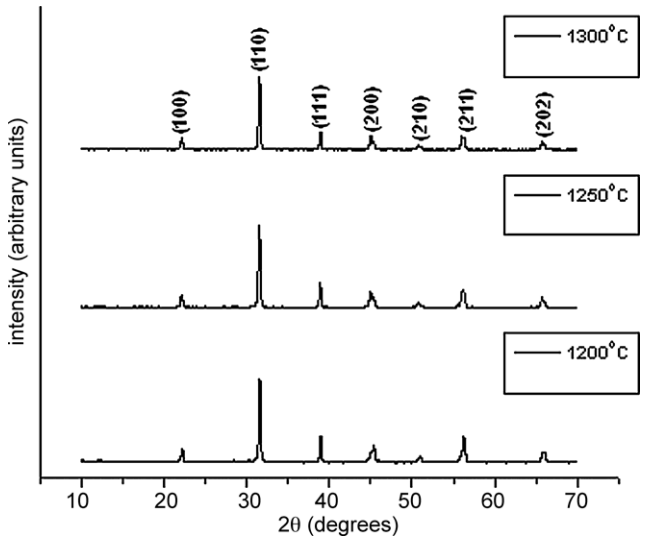

Fig. 1. X-ray diffractograms of $BaZr_{0.025}Ti_{0.975}O_3$ ceramics sintered at 1200 °C, 1250 °C and 1300 °C.

and refined using least square refinement method by a computer programme package Powder-X. They reveal the formation of perovskite structure with tetragonal phase in the compound. It is observed that the diffraction peaks shift towards the lower angle with the increase in sintering temperature. This is possibly due to the fact that the ionic radius of Zr^{+4} ion (0.87 Å) is higher than that of Ti^{+4} ion (0.68 Å) and more and more Zr^{+4} ions occupy Ti^{+4} sites on increasing the sintering temperature [17]. Moreover, the splitting of tetragonal peaks (1 0 0) and (0 0 1); (2 0 0) and (0 0 2); and (2 1 0) is observed at $2\theta = 22.355°$, 45.262°, 51.096° respectively on increasing the sintering temperature which is indicative of the fact that the tetragonal phase grows when the sample is sintered at higher temperature [18].

3.2. Surface morphology

Fig. 2 shows the SEM micrographs of BZT ceramics sintered at temperatures 1200 °C, 1250 °C and 1300 °C. The specimen sintered at 1200 °C has small grains and a porous microstructure. On increasing the sintering temperature well developed grains with uniform grain distribution is observed. The average grain size is observed to be 0.62 μm, 2.82 μm and 3.20 μm respectively in the samples sintered at 1200 °C, 1250 °C and 1300 °C. The grain size in the samples increases as the sintering temperature is increased. The driving force responsible for the increase in grain size is proportional to the difference between free energy of the strained matrix and the strain free crystals and hence the larger grain size results from the decrease in grain boundary area and the total boundary energy [19]. When the grain size increases there is reduction in porosity and hence when there is adjoining of grains, the driving force for the grain boundary migration and pore shrinkage reduces to zero [20]. Also the domain structures are clearly seen in the SEM micrographs. The domain structures appear in the high resolution SEM in these compounds which has been earlier reported by Wei Cai et al. [17]. In the present work also the domains are visible. The domains with "lamellar" and water-mark characters are observed as indicated in Fig. 2 by circles A, B, C, D, and E. The increase in grain size can also be attributed to lower interfacial energy and the interfacial energy is inversely proportional to the grain diameter [21].

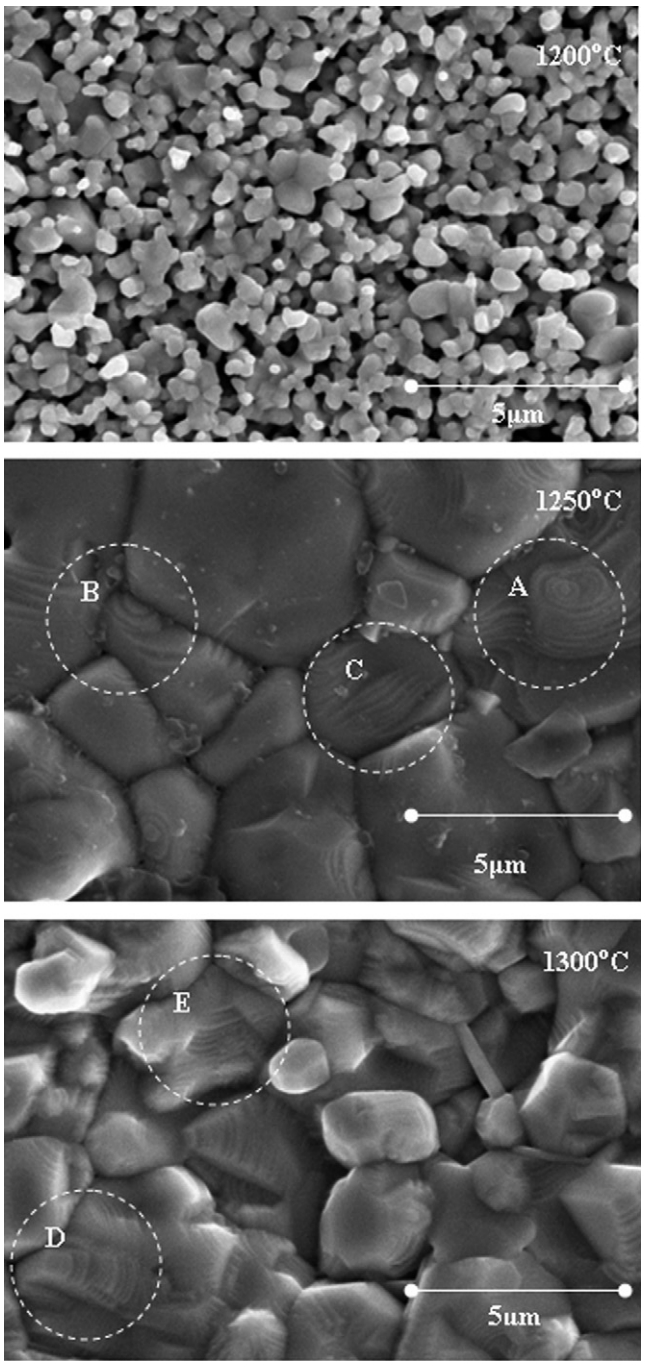

Fig. 2. SEM micrographs of $BaZr_{0.025}Ti_{0.975}O_3$ ceramics sintered at 1200 °C, 1250 °C and 1300 °C.

3.3. Dielectric study

Fig. 3 shows the temperature dependence of dielectric constant of the studied specimens at 1 kHz, 10 kHz and 100 kHz frequency. The figures show that the value of permittivity increases gradually to a maximum value (ε_m) with increase in temperature up to the transition (Curie) temperature and then decreases gradually indicating a phase transition. A diffuse phase transition on substitution of zirconium [22] is observed. There is an enormous increase in dielectric constant from 540.586 in the sample sintered at 1200 °C to 3208.581 and 4840.437 in the samples sintered at 1250 °C and 1300 °C respectively at 1 kHz which may be attributed to increasing space charge (i.e. oxygen vacancies) with increasing sintering

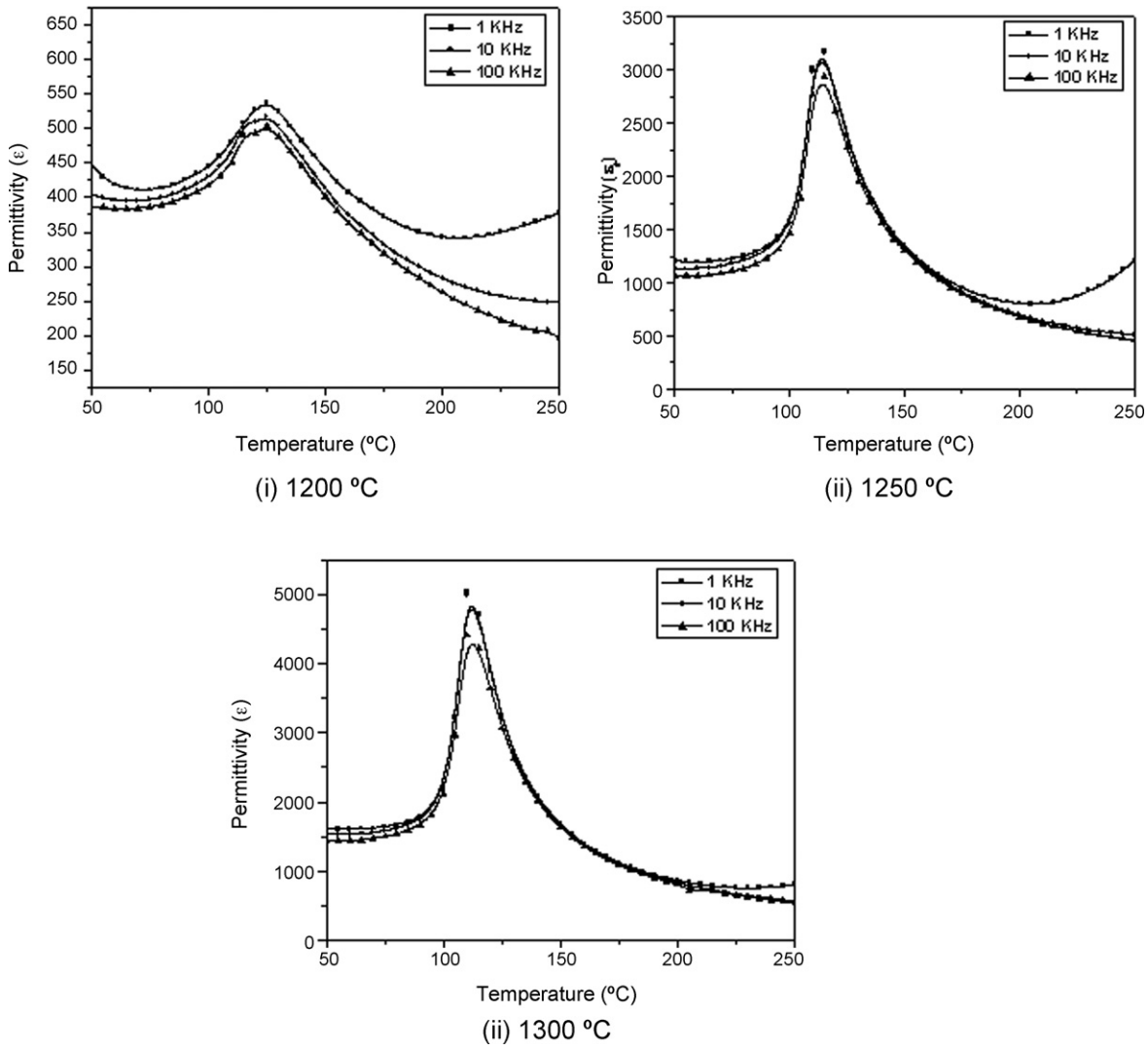

Fig. 3. Variation of permittivity with temperature at frequencies 1 kHz, 10 kHz and 100 kHz (i) 1200 °C (ii) 1250 °C (iii) 1300 °C.

temperature which leads to enhanced space charge polarization subsequently leading to the higher dielectric constant. There is broad permittivity temperature curve in the transition temperature region as seen in Fig. 3, which can be attributed to inhomogeneous distribution of Zr ions at the Ti sites [23] due to the higher ionic radius of zirconium ion. The broad permittivity–temperature curve can also be attributed to the tolerance factor of the perovskite structure. For perovskites with the general formula of ABO_3, the following equation is used to calculate the tolerance factor, t [24]:

$$t = \frac{R_O + R_A}{\sqrt{2}(R_B + R_O)} \quad (1)$$

where R_A is the radius of A-site atom, R_B that of the B-site atom and R_O that of the O atom.

For the composition in the present work, the above equation can be rewritten as:

$$t = \frac{R_O + R_{Ba^{+2}}}{\sqrt{2}(xR_{Zr^{+4}} + (1-x)R_{Ti^{+4}} + R_O)} \quad (2)$$

For a stable perovskite structure, value of t should be unity. The normal ferroelectric phase gets stabilized in barium titanate [25]. The calculated value of tolerance factor with the present composition is 0.92. Thus the substitution of Zr^{+4} at Ti^{+4} sites destabilizes the

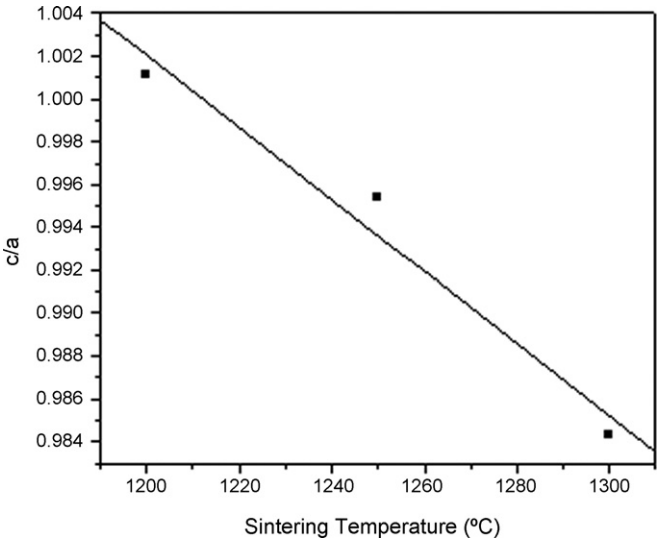

Fig. 4. Variation of tetragonal strain (c/a) with sintering temperature.

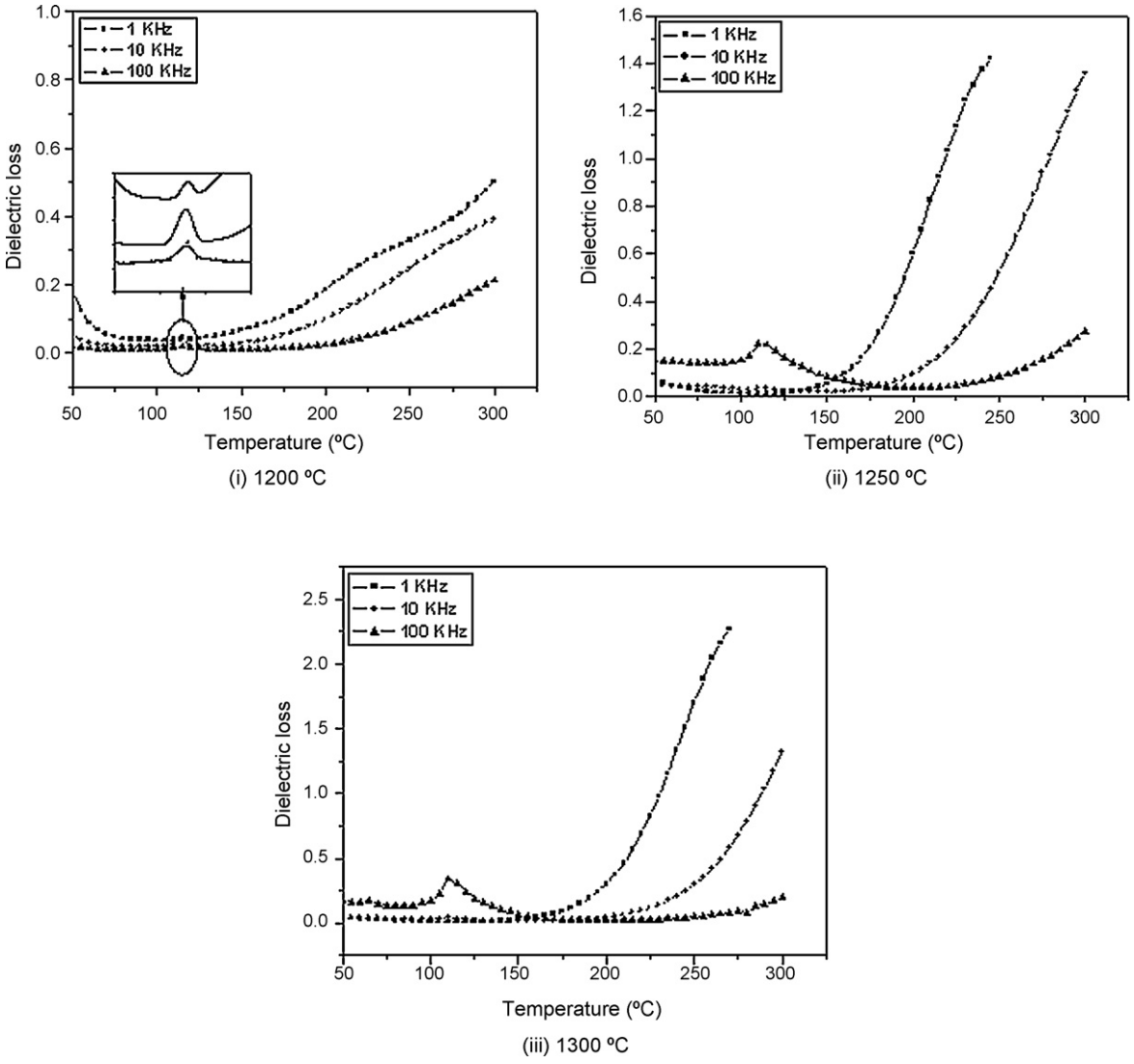

Fig. 5. Variation of dielectric loss tan δ with temperature at frequencies 1 kHz, 10 kHz and 100 kHz (i) 1200 °C (ii) 1250 °C (iii) 1300 °C.

normal ferroelectric structure and induces paraelectric behavior due to the higher ionic diameter and lower polarization.

It is observed that the permittivity increases with increase in sintering temperature. This can be understood as follows: at the higher sintering temperature the average grain size increases making the domain wall motion easier resulting in an increased dielectric constant [26]. As the sintering is carried out in air, reoxidation will take place around the grains during the cooling process. Hence the lattice can pick up oxygen from the surroundings and reoxidation results in a strong insulating layer around a grain with a higher bulk resistance leading to the high interfacial polarization and increase in dielectric constant [27]. As the behavior of grain boundary is responsible for the large resistance and capacitance compared to the grain interior [28,29]. The difference in the conductivity of the bulk and grain boundary results in an increase in surface charge accumulation and this in turn, results in an increase of interfacial polarization. It is also observed that T_c reduces on substitution of zirconium from 125 °C to 120 °C and 115 °C as the sintering temperature is increased. This is possibly due to the higher ionic radii of Zr^{+4} than Ti^{+4}. Substitution of Zr^{+4} for Ti^{+4} weaken the bonding force between the Ti^{+4} and the oxygen ion of the ABO_3 perovskite structure. As the Zr–O bonds (776.1 kJ/mol) are stronger than Ti–O bonds (672.4 kJ/mol), hence the Zr^{+4} ions can be substituted at lower temperature for cubic phase formation, hence the phase transition temperature is reduced [30]. On the other hand, the weakening of Ti–O bond leads to a weaker distortion of the octahedron and the substitution of Zr might induce a "break" of the cooperative vibration of Ti–O chains; this could bring about a decrease in the c/a ratio as depicted in Fig. 4. This "break" is responsible for the drop in Curie temperature [31,32].

The dielectric loss of the studied samples from room temperature to 300 °C is shown in Fig. 5. At lower frequencies it is observed that the loss is independent of temperature up to nearly 200 °C and then rapidly increases with increase in temperature. This sharp increase of dielectric loss in high temperature region may be attributed to the increased mobility of charge carriers arising from defects or vacancies in the sample [33]. This behavior can also be attributed to the domain boundary vibrations or excitations that are readily stimulated under the weak a.c. drive conditions [34]. The loss peaks at 1 kHz frequency are associated with the phase transitions. It is observed that loss peaks are not formed at higher frequencies. This can be understood as follows: at some suitable frequencies of the applied alternating field, resonance in dielectric behavior is often observed [35]. At higher frequencies, the dipoles cannot keep up with the applied alternating field, their amplitude of

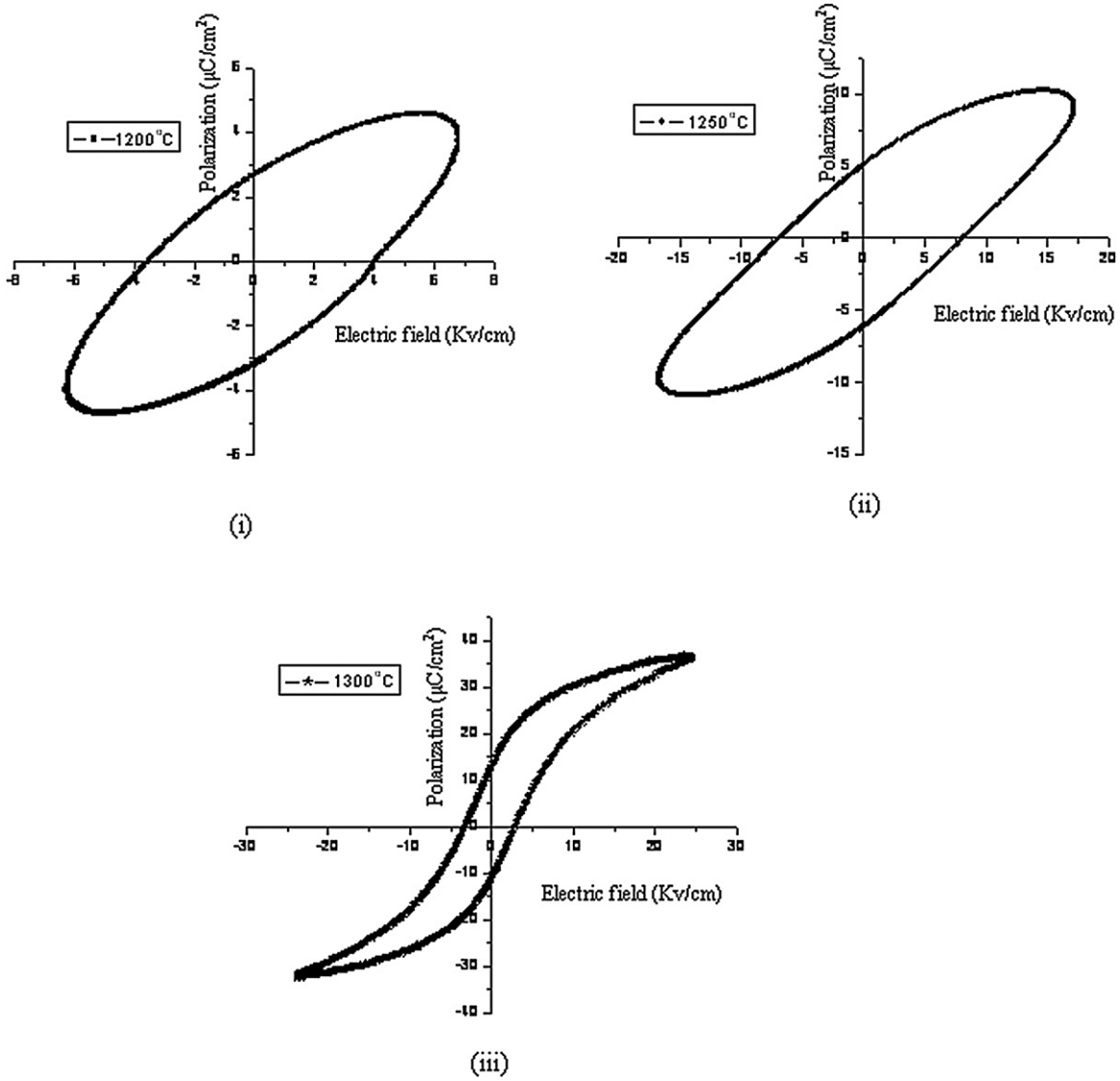

Fig. 6. Ferroelectric hysteresis loops showing remanent polarization (P_r) and coercive field (E_c) at (i) 1200 °C (ii) 1250 °C (iii) 1300 °C.

vibration will not be correlated and hence the polarization cannot follow the applied alternating field [20].

3.4. Hysteresis loops

Fig. 6 shows the hysteresis loops of the studied specimens measured at room temperature. The *P–E* hysteresis loop is unsaturated in the sample sintered at lower temperature leading to poor ferroelectricity [36]. The remanent polarization ($2P_r$) increases from 4 μC/cm^2 to 10 μC/cm^2 and then to 24 μC/cm^2 with the increase in sintering temperature. There are two major effects of grain boundary on polarization. As the grain size is small leading to large number of grain boundaries [17] and it is well known that grain boundary is a low permittivity region, hence poor ferroelectricity. On the other hand there is polarization discontinuity between grain boundary and grain surface and hence polarization ($2P_r$) decreases. It is also seen that coercive field decreases with increase in sintering temperature. This is due to the fact that energy barrier for switching ferroelectric domain gets reduced as the grain size increases. Polarization reversal of a ferroelectric domain is much easier inside a larger grain compared to that in a smaller grain.

4. Conclusions

The synthesized compounds are formed with perovskite structure in tetragonal phase. As the sintering temperature increases from 1200 °C to 1250 °C and 1300 °C, the average grain size increases from 0.62 μm to 2.82 μm and 3.20 μm. The domain structures with water-mark and lamellar features are seen in the SEM micrographs. A diffuse phase transition is observed in the studied specimens. The dielectric constant increases with increase in average grain size in the specimens. The substitution of zirconium leads to the decrease of Curie temperature. The dielectric loss is independent of temperature nearly up to 200 °C and then rapidly increases with increase in temperature. The loss peaks are attributed to the phase transitions and consequent dissolution of domains. The coercive field decreases and remanent polarization increases with increase in grain size of the specimens. At higher sintering temperature the value of remanent polarization increases considerably.

References

[1] J. Zhai, D. Hu, Xi. Yao, Z. Xu, H. Chen, J. Eur. Ceram. Soc. 26 (2006) 1917.
[2] X. Tang, X.X. Wang, K.H. Wong, H.L.W. Chan, Appl. Phys. A 81 (2009) 1253.

[3] Z. Jiwei, Y. Xi, Z. Liangying, S. Bo, H. Chen, J. Cryst. Growth 262 (2004) 341.
[4] X.G. Tang, R.K. Zheng, Y.P. Jiang, H.L.W. Chan, J. Phys. D: Appl. Phys. 39 (2006) 3394.
[5] G.H. Haertling, J. Am. Ceram. Soc. 82 (1999) 797.
[6] R.E. Jones, P.D. Mainar, J.O. Olowolafe, J.O. Campbell, C.J. Mogab, Appl. Phys. Lett. 60 (1992) 1022.
[7] M.H. Frey, D.A. Payne, Appl. Phys. Lett. 63 (1963) 2753.
[8] H. Hu, S.B. Krupanidhi, J. Appl. Phys. 74 (1993) 3373.
[9] D.R. Lide, CRC Handbook of Physics and Chemistry, 88th ed., (2007) CRC Press.
[10] J.W. Zhai, X. Yao, L.Y. Zhang, B. Shen, Appl. Phys. Lett. 84 (16) (2004) 3136.
[11] X.G. Tang, K.H. Chew, H.L.W. Chan, Acta Mater. 52 (17) (2004) 5177–5183.
[12] X.P. Jiang, M. Zeng, H.L.W. Chan, et al., Mater. Sci. Eng. A 438–440 (2006) 198–201.
[13] A. Mukherjee, P. Victor, J. Parui, et al., J. Appl. Phys. 101 (3) (2007), 034106: 1–6.
[14] X.G. Tang, Q.X. Liu, Y.P. Jiang, et al., J. Appl. Phys. 100 (2006) 114105.
[15] S.K. Rout, Phase formation and dielectric studies of some BaO–ZrO–TiO perovskite systems, Ph.D. Thesis.
[16] Chen Yunfei, R. Lukes Jennifer, Li Deyu, Yang Juekuan, Wu Yonghua, J. Chem. Phys. 120 (8) (2004) 3841–3846.
[17] Wei Cai, Chunlin Fu, Jiacheng Gao, Huaqiang Chen, J. Alloys Compd. 480 (2009) 870–873.
[18] S. Devi, A.K. Jha, Physica B 404 (2009) 4290–4294.
[19] W.D. Kingrey, Introduction to Ceramics, Wiley, New York, 1960.
[20] M.W. Barsoum, Fundamentals of Ceramics, McGraw Hill, 1997.
[21] J. Tullis, R.A. Yund, J. Geol. 90 (3) (1982) 301–308.
[22] D. Hennings, A. Schnell, G. Simon, J. Am. Ceram. Soc. 65 (1982) 539.
[23] U. Weber, G. Greuel, U. Boettger, S. Weber, D. Hennings, R. Waser, J. Am. Ceram. Soc. 84 (2004) 759.
[24] S.K. Rout, E. Sinha, S. Panigrahi, Mater. Chem. Phys. 101 (2007) 428.
[25] H.T. Martirena, J.C. Burfoot, J. Phys. C: Solid State Phys. 7 (1976) 3162.
[26] S. Bhaskar Reddy, K. Prasad Rao, M.S. Ramachandra Rao, Appl. Phys. Lett. 91 (2007) 022917.
[27] D.C. Sinclair, A.R. West, J. Appl. Phys. 66 (1989) 3850.
[28] D.C. Sinclair, T.B. Adams, F.D. Morrison, A.R. West, Appl. Phys. Lett. 80 (2002) 2153.
[29] D. Henning, A. Schnell, G. Simon, J. Am. Ceram. Soc. 65 (1982) 539.
[30] S.G. Lee, D.S. Kang, Mater. Lett. 57 (2002) 1629.
[31] W.R. Huo, Y.F. Qu, Sens. Actuators A 128 (2006) 265.
[32] N. Sawangwan, J. Barrel, K. Mackenzie, T. Tunaksiri, Appl. Phys. A 90 (2008) 723.
[33] P. Ganguly, A.K. Jha, J. Alloys Compd. 495 (2010) 7–12.
[34] X. Zong, Z. Yang, H. Li, M. Yuan, Mater. Res. Bull. 41 (2006) 1447.
[35] R.C. Buchanan, Ceramic Materials for Electronics: Processing, Properties and Applications, Marcel Dekker, Inc., New York, 1991.
[36] N. Nanakorn, P. Jalupoom, N. Vaneesorn, A. Thanaboonsombut, Ceram. Int. 34 (2008) 779–782.